Contribution from the Department of Chemistry,
State University of New York, Buffalo, New York 14214

# The Ferro/Ferricyanide Couple in an Aluminum Chloride–1-Methyl-3-ethylimidazolium Chloride Ambient-Temperature Molten Salt

B. Das,† R. Carlin, and R. A. Osteryoung*

*Received April 26, 1988*

Tetrabutylammonium ferricyanide, $(Bu_4N)_3Fe(CN)_6$, has been prepared and investigated in the 1-methyl-3-ethylimidazolium chloride–aluminum chloride (ImCl–$AlCl_3$) ambient-temperature molten salt solvent. The voltammetry and UV–visible spectroscopy of $(Bu_4N)_3Fe(CN)_6$ have been compared to those of $K_3Fe(CN)_6$ in water and are shown to be identical; in addition, the molecular weight of $(Bu_4N)_3Fe(CN)_6$ has been determined by an electroanalytical method and is in good agreement with that expected. $(Bu_4N)_3Fe(CN)_6$ is insoluble in the basic ImCl–$AlCl_3$ melt but is soluble in the acidic melt. However, the ferricyanide reacts to form the ferrocyanide species; i.e., the oxidation potential of the ferro/ferricyanide couple is sufficiently positive to oxidize chloride from tetrachloroaluminate. Spectral shifts observed for the molten salt suggest that $AlCl_3$ forms adducts with the ferrocyanide, which accounts for the large positive shift in the oxidation potential of the ferro/ferricyanide redox couple relative to that in water. The ferro/ferricyanide couple could be examined voltammetrically at a carbon, but not at a platinum, electrode since the tetrachloroaluminate oxidation is significantly more irreversible on the former than the latter, and the formal potential was estimated as +2.30 V vs an Al reference in the 1.5:1 molten salt.

## Introduction

Ambient-temperature molten salts consisting of $AlCl_3$ and an organic chloride are of considerable interest as solvents for a variety of electrochemical and spectroscopic studies.[1,2] One such solvent, aluminum chloride–1-methyl-3-ethylimidazolium chloride ($AlCl_3$–ImCl), is a liquid at room temperature over the composition range 33–67 mol % $AlCl_3$.[3,4] The solvent shows Lewis acidity and basicity depending upon the $AlCl_3$:ImCl mole ratio. If the ratio is greater than, equal to, or less than 1, the solvent is acidic, neutral, or basic, respectively. Electrochemical and spectroscopic studies of organic[5,6] and inorganic[7-10] solutes have been carried out in these solvents.

Here we describe spectrochemical and electrochemical studies on the ferricyanide/ferrocyanide couple in the $AlCl_3$–ImCl molten salt solvent.

## Experimental Section

Ferricyanide and ferrocyanide with their common counterions, $K^+$ or $Na^+$, are insoluble in the $AlCl_3$–ImCl melt over the entire acidity range. Salts containing quaternary ammonium cations have a favorable solubility in the melt; potassium ferricyanide was, therefore, converted to tetrabutylammonium ferricyanide, $(Bu_4N)_3Fe(CN)_6$, by treatment with tetrabutylammonium chloride.

Potassium ferricyanide (J. T. Baker Chemical Co.) and tetrabutylammonium chloride (Sigma Chemical Co.) were added in a molar ratio of ca. 1:3 to a 50:50 v/v mixture of methylene chloride (Fisher Scientific, Certified ACS grade) and distilled water. The mixture was stirred for about 2 h and the organic layer collected. The solvent was evaporated and the yellow residue containing $(Bu_4N)_3Fe(CN)_6$ and $(Bu_4N)Cl$ dried under vacuum. Diethyl ether (Baker Chemical Co., USP) was added to the residue, and the mixture was stirred for several hours, then boiled for 5–10 min, and filtered while hot. The operation was repeated. Tetrabutylammonium chloride was removed in ether solution and $(Bu_4N)_3Fe(CN)_6$ obtained as the residue. The product was dried in an oven at 100 °C and analyzed voltammetrically (see below) and spectroscopically.

Tetrabutylammonium ferrocyanide, $(Bu_4N)_4Fe(CN)_6$, however, could not be synthesized from potassium ferrocyanide by following the same procedure. In the water–methylene chloride solvent, the distribution of tetrabutylammonium ferrocyanide in the organic layer was found to be very small in comparison to that of tetrabutylammonium chloride. Moreover, in the separation step with diethyl ether the entire residue was soluble, which prevented the isolation of the small amount of tetrabutylammonium ferrocyanide.

1-Methyl-3-ethylimidazolium chloride (ImCl) was synthesized by following known procedures[3] and aluminum chloride (Fluka AC, iron free) purified by sublimation. A melt of particular acidity was prepared by mixing the requisite weighed quantities of the two salts. The acidity of the solution was changed by adding either $AlCl_3$ or ImCl. All electrochemical measurements in the melt were performed in a Vacuum Atmospheres Co. drybox under purified helium at a temperature of 26 ± 2 °C.

UV–vis spectra were taken on a Varian Model Cary 118 spectrophotometer using a 1-mm quartz cell (Starna Cell Inc.). A Mattson Instruments Alpha Centauri FTIR spectrometer connected to an AT&T PC 7300 computer and a Graphtec WX 4731 PLOTWRITER was used for IR spectra. The sample was taken in a Spectra-Tec sealed precision path length cell with $CaF_2$ or NaCl windows and a 0.025-mm Teflon spacer; the cell was filled with the sample in the drybox, sealed, and then taken to the spectrometer.

Cyclic voltammetric studies were performed with an EG&G PARC Model 175 universal programmer in combination with a Model 173 potentiostat/galvanostat. Voltammograms were plotted on a Houston Instruments Model 200 X-Y recorder. All other electrochemical studies were done with an EG&G PARC Model 273 potentiostat/galvanostat controlled by a DEC PDP-8/e computer. Plots were obtained from a DEC LA50 system connected to the computer.

Rotating-disk voltammetry was performed by using a Pine Instrument Co. glassy-carbon ring-disk electrode (disk radius 0.4 cm) and a Pine ASR rotator.

**Table I.** Calibration Data for Determination of $(Bu_4N)_3Fe(CN)_6$ Molecular Weight[a]

| $[K_3Fe(CN)_6]$, mM | mg of $(Bu_4N)_3Fe(CN)_6$/mL of soln[b] | $i_{p_a}$, μA | $i_{p_a}/C$ |
|---|---|---|---|
| 3.85 | | 15.0 | 3.90 |
| 5.66 | | 22.3 | 3.93 |
| 7.41 | | 29.3 | 3.94 |
| 9.09 | | 35.3 | 3.88 |
| 10.71 | | 41.5 | 3.87 |
| | | | 3.90 (av) |
| | 20.4/4.00 | 21.3 | |

[a] Pt working electrode ($r$ = 0.08 cm); supporting electrolyte 0.5 M KCl. [b] The concentration of the $(Bu_4N)_3Fe(CN)_6$ solution obtained from the calibration curve is 5.45 mM, which amounts to 2.18 μmol of the substance in 20.4 mg, giving a molecular weight of 936.

† Present address: Department of Chemistry, University of Rajshahi, Rajshahi, Bangladesh.

(1) Hussey, C. L. *Adv. Molten Salt Chem.* **1983**, *5*, 185.
(2) Osteryoung, R. A. In *Molten Salt Chemistry*; Mamantov, G., Morassi, R., Eds.; NATO ASI Series, Vol. 202; Reidel: Boston, MA, 1987, p 329.
(3) Wilkes, J. S.; Levisky, J. A.; Wilson, R. A.; Hussey, C. L. *Inorg. Chem.* **1982**, *21*, 1263.
(4) Wilkes, J. S.; Levisky, J. A.; Pflug, J. L.; Hussey, C. L.; Sheffler, T. B. *Anal. Chem.* **1982**, *54*, 2378.
(5) Gale, R. J.; Gilbert, B.; Osteryoung, R. A. *Inorg. Chem.* **1978**, *17*, 2728.
(6) Robinson, J.; Osteryoung, R. A. *J. Am. Chem. Soc.* **1980**, *102*, 4415.
(7) Gale, R. J.; Gilbert, B.; Osteryoung, R. A. *Inorg. Chem.* **1979**, *18*, 2723.
(8) Hussey, C. L.; Laher, T. M. *Inorg. Chem.* **1981**, *20*, 4201.
(9) Linga, H.; Stojeck, Z.; Osteryoung, R. A. *J. Am. Chem. Soc.* **1981**, *103*, 3754.
(10) Hussey, C. L.; King, L. A.; Wilkes, J. S. *J. Electroanal. Chem. Interfacial Electrochem.* **1979**, *102*, 321.

0020-1669/89/1328-0421$01.50/0 

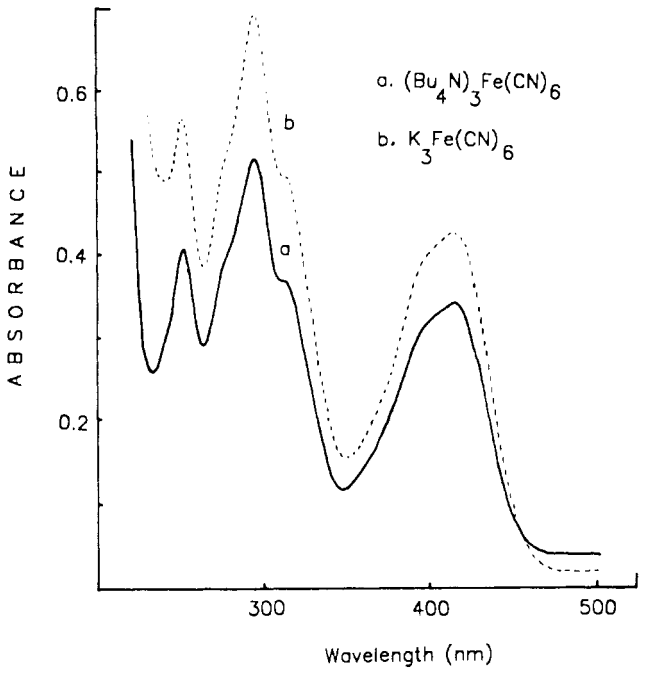


**Figure 1.** UV–vis absorption spectra of (a) $[(C_4H_9)_4N]_3Fe(CN)_6$ and (b) $K_3Fe(CN)_6$ in aqueous media (scan rate 1 nm/s; slit 0.3 nm).

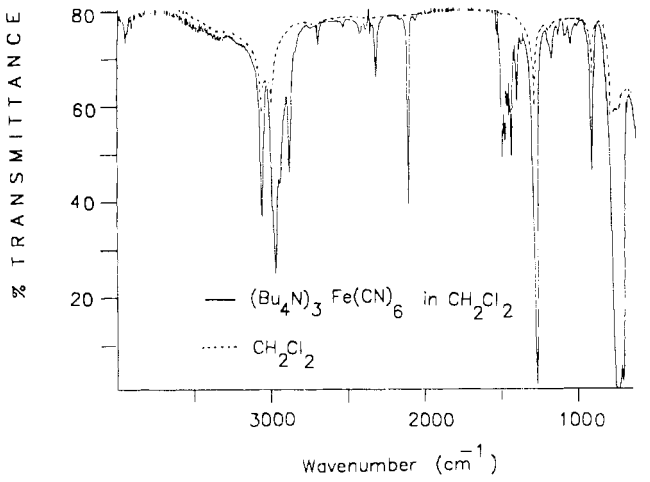


**Figure 2.** FTIR spectra of $[(C_4H_9)_4N]_3Fe(CN)_6$ in $CH_2Cl_2$ (—) and $CH_2Cl_2$ (- - -) (resolution 2 $cm^{-1}$).

The working electrodes were Pt ($r$ = 0.08 cm) or glassy carbon, GC ($r$ = 0.15 cm), from Bioanalytical Systems Inc. and a tungsten disk made in the laboratory by heat-sealing a wire (Alfa Products, Morton Thiokol Inc.; $r$ = 0.025 cm) into glass. For all electrochemical measurements in the melt, the reference electrode was an Al wire (5N Alfa Inorganics) immersed in a solvent of 1.5 mole ratio $AlCl_3$:ImCl in a fritted-glass tube; the counter electrode was a coiled Al wire of the same origin. Unless otherwise stated, all potentials are reported with respect to the above reference.

## Results and Discussion

**1. Analysis of Tetrabutylammonium Ferricyanide.** The cyclic voltammograms and UV–vis spectra of the synthesized $(Bu_4N)_3Fe(CN)_6$ and Baker's $K_3Fe(CN)_6$ were compared. The cyclic voltammograms of both compounds in 0.5 M KCl solution appeared to be identical, having the same $E_{p_a}$ and $E_{p_c}$ values. Figure 1 compares the UV–vis spectra of the two compounds. The shape and peak positions show that $(Bu_4N)_3Fe(CN)_6$ contains ferricyanide. The molecular weight of the compound was determined by calibration using cyclic voltammetry with $K_3Fe(CN)_6$ as a standard and was calculated to be 936.[11] Results are shown in Table I. The formula weight for $(Bu_4N)_3Fe(CN)_6$ is 938.

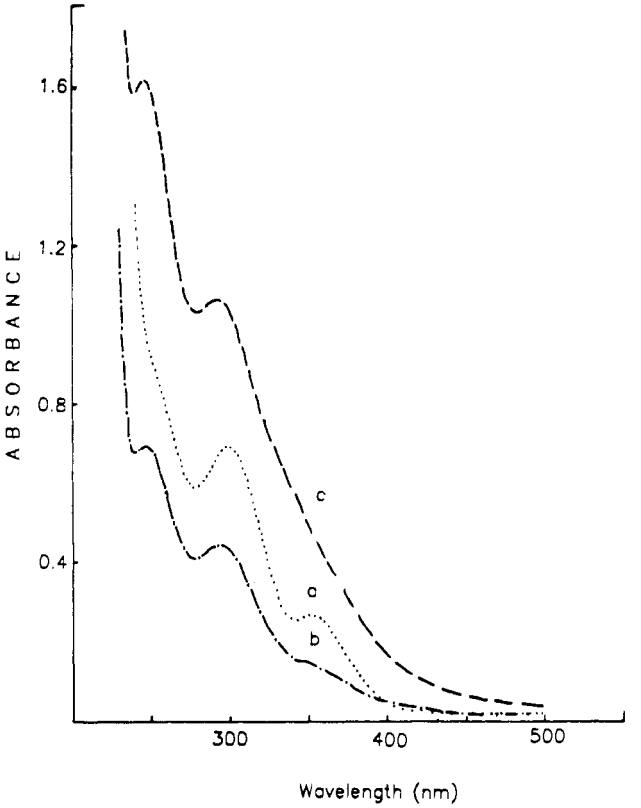


**Figure 3.** UV–vis absorpiton spectra of $[(C_4H_9)_4N]_3Fe(CN)_6$ in (a) slightly acidic $AlCl_3$:ImCl, (b) 1.2:1 $AlCl_3$:ImCl, and (c) 1.5:1 $AlCl_3$:ImCl melts (scan rate 1 nm/s; slit 0.3 mm).

Additional evidence for the composition of $(Bu_4N)_3Fe(CN)_6$ is obtained from the IR spectrum of the compound in $CH_2Cl_2$ (Figure 2); a sharp band at 2100 $cm^{-1}$, in addition to others at 2966, 2940, and 2876 $cm^{-1}$, and groups of closely spaced bands in the regions 1480–1380 and 1150–1000 $cm^{-1}$, is found.

The band at 2100 $cm^{-1}$ compares favorably with the reported C–N stretch of $K_3Fe(CN)_6$ in water at 2118 $cm^{-1}$.[12] Considering the possibility of the formation of a weak adduct between $H_2O$ and $Fe(CN)_6^{3-}$ through the N of C–N, the 18-$cm^{-1}$ positive shift of the band position relative to that in $CH_2Cl_2$ is reasonable.[13-15] The bands at 2966, 2940, and 2876 $cm^{-1}$ are attributable to the C–H stretch in the alkyl groups. The bands in the region 1480–1380 $cm^{-1}$ correspond to the C–H bending vibrations, and those in the 1150–1000-$cm^{-1}$ region arise, in part, from C–N stretching vibrations in the quaternary ammonium ion.[16]

**2. Spectroscopy on $(Bu_4N)_3Fe(CN)_6$ in the $AlCl_3$–ImCl Melt.** Solid $(Bu_4N)_3Fe(CN)_6$ is yellow; the salt is insoluble in the neutral or basic melt. Stirring the mixture for several hours results in a yellow colloid, which was not found to undergo any further change, even after 1 month. It is, however, soluble in the acid melt.

The color of the slightly acidic solution is light brown and becomes darker with increasing acidity. It is shown (see below) that ferricyanide is unstable and is reduced to ferrocyanide in the acid melt. The slightly acidic melt shows absorption bands at 357 and 306 nm in the UV–vis spectrum (Figure 3a). When the acidity of the solution is increased to a 1.2:1 $AlCl_3$:ImCl ratio, the bands shift to 303 and 257 nm, leaving a small shoulder at 357 nm (Figure 3b). Increasing the acidity further to 1.5:1 only removes the shoulder at 357 nm, but the other bands remain

(11) Bard, A.; Faulkner, L. R. *Electrochemical Methods*; Wiley: New York, 1980; Chapter 6.
(12) Jones, L. H. *Inorg. Chem.* **1963**, *2*, 777.
(13) Shriver, D. F. *J. Am. Chem. Soc.* **1963**, *85*, 1405.
(14) Shriver, D. F.; Posner, J. *J. Am. Chem. Soc.* **1966**, *88*, 1672.
(15) Woodcock, C.; Shriver, D. F. *Inorg. Chem.* **1986**, *25*, 2137.
(16) Pouchart, C. J. *The Aldrich Library of Infrared Spectra*, 3rd ed.; Aldrich Chemical Co.: Milwaukee, WI; pp 1–2, 163–164.

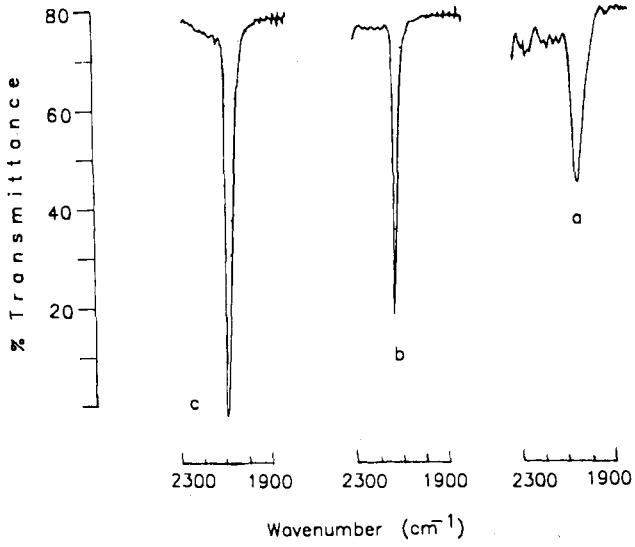


**Figure 4.** FTIR spectra of $[(C_4H_9)_4N]_3Fe(CN)_6$ in (a) slightly acidic $AlCl_3$:ImCl, (b) 1.2:1 $AlCl_3$:ImCl, and (c) 1.5:1 $AlCl_3$:ImCl melts (resolution 2 $cm^{-1}$).

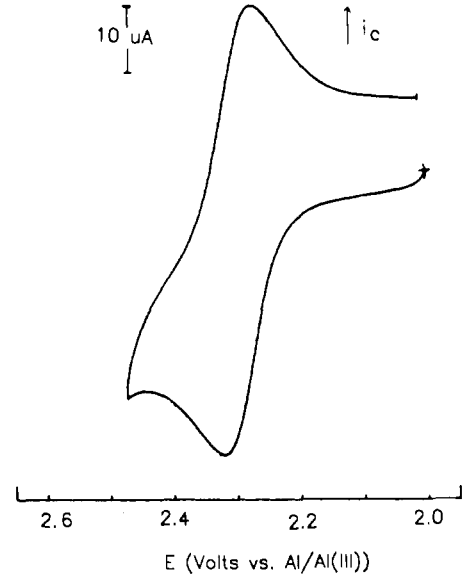


**Figure 5.** Cyclic voltamogram of 18.92 mM $[(C_4H_9)_4N]_3Fe(CN)_6$ in 1.5:1 $AlCl_3$:ImCl melt (scan rate 50 mV/s; GC electrode ($r$ = 0.15 cm); reference electrode Al/Al(III) in 1.5:1 $AlCl_3$:ImCl melt).

unchanged (Figure 3c). When the solution acidity is lowered from 1.5:1, the spectral features indicated above are retraced. This suggests that the complex is stable in the melt. The UV–vis bands in an aqueous solution of ferrocyanide are at 422, 322, and 270 nm.[17] An examination of the spectra suggests that the bands at 422 and 322 nm in the aqueous solution are blue-shifted in the slightly acidic melt to 357 and 306 nm and are further blue-shifted to 303 and 257 nm at 1.2:1 and higher acidity ratios. The third band has most probably moved into the melt cutoff. Similar shifts have been reported for $Fe(phen)_2(CN)_2$ spectra in acidic chloroaluminate melts referenced to their spectra in $CH_2Cl_2$.[15] The UV–vis bands are due to the d–d transitions of the central metal.[17] Considering that the adduct formation of the complex with $AlCl_3$ through the N of the CN groups increases the order of the M–C $\pi$ bond and stabilizes the ground state of the metal ion,[14] the blue shift of the bands of d–d transitions and their increase with acidity is reasonable.

Similar behavior is observed in the IR band corresponding to the C–N stretch (Figure 4). In a slightly acidic melt, the band occurs at 2108 $cm^{-1}$; this band shifts to 2125 $cm^{-1}$ in 1.2:1 melts and remains constant at that value with further increase of acidity. Relative to the C–N stretching band in an aqueous solution of ferrocyanide at 2044 $cm^{-1}$,[12] the band in a 1.2:1, or more acidic, $AlCl_3$–ImCl melt is 82 $cm^{-1}$ higher. This shift of the C–N stretching band is comparable to that observed by Shriver and co-workers[13,14] for the metal cyano complex adducts with $BF_3$ and to that in an acid chloroaluminate melt[15] and perhaps indicates the formation of adducts such as Fe–CN·$AlCl_3$, as previously suggested.[15] The single sharp band in the acid melt futher suggests that the adducts are formed equally with all the CN groups.

When the acid-melt solution is made basic (0.8:1 $AlCl_3$:ImCl), it again becomes colloidal, but the color is much lighter than that obtained by attempting to dissolve $(Bu_4N)_3Fe(CN)_6$ in the basic melt. Since the colloid now contains ferrocyanide, rather than ferricyanide, the lighter color is expected.

**3. Electrochemistry of Tetrabutylammonium Ferricyanide in an AlCl–ImCl Melt.** As stated above, $(Bu_4N)_3Fe(CN)_6$ forms a colloid in neutral and basic melts. No electroactivity of the colloid could be observed. In the acid melt, no electroactivity at a Pt electrode was found up to +2.2 V, the limit of the anodic window of the acid melt. However, at GC and W electrodes chloride discharge in the acid melt has a larger overvoltage than at Pt, which permitted these electrodes to be used in the investigation. The equilibrium potential of a solution containing added $(Bu_4N)_3Fe(CN)_6$ in a 1.5:1 $AlCl_3$–ImCl melt was +1.95 V. Both anodic and cathodic currents were obtained by cyclic voltammetry with a peak separation of about 75 mV at 50 mV/s scan rate (Figure 5). The formal potential of the couple calculated from the voltammogram was +2.30 V. This behavior indicates that the solution contained the reduced form of the couple, although it was initially prepared from the ferricyanide salt.

We considered as a possibility that (i) the cyclic voltammogram corresponds to the Fe(IV)/Fe(III) couple, (ii) the ferricyanide has decomposed, or (iii) the ferricyanide is reduced to ferrocyanide and the cyclic voltammogram represents the Fe(III)/Fe(II) cyano complexes.

We expect that an Fe(IV) cyano complex would be extremely unstable, and furthermore, no electroactivity corresponding to the reduction of ferricyanide was observed at potentials more negative than 2.2 V; thus, the first possibility is unlikely. As to the second, the most probable decomposition product of ferricyanide is Fe(III), whose electrochemical behavior differs markedly from that of the present system.[18] On the other hand, the formal potential of the couple indicates that ferricyanide will be thermodynamically unstable with respect to the oxidation of tetrachloroaluminate and will be reduced to ferrocyanide. There is also other evidence in support of the presence of ferrocyanide in the solution. When water was added to the acid-melt solution containing added $(Bu_4N)_3Fe(CN)_6$ in the presence of air, the solution color turned Prussian blue, a behavior that is shown by ferrocyanide in acid medium.[19]

The large positive shift of oxidation potential of ferrocyanide in the acid melt is a consequence of the enhanced stability of the ground state of Fe(II) due to the adduct formation of the complex with $AlCl_3$. With the electron-accepting ability of the solvent, the ground state of the central metal ion of the complex becomes increasingly more stable, leading to an increase of its oxidation potential. Gutmann et al.[20,21] have obtained a positive shift of about +1.2 V in the oxidation potential of ferrocyanide in going from *N,N'*-dimethylformamide to water. Thus, in our strongly Lewis acid system, the increase in potential of about +2 V relative to that in water is not unreasonable. Woodcock and Shriver[15] have shown a shift for the oxidation of $Fe(phen)_2(CN)_2$ of ca. +0.8 V in the acidic chloroaluminates compared to methylene chloride.

(17) Gray, H. B.; Beach, N. A. *J. Am. Chem. Soc.* **1963**, *85*, 2922.

(18) Nanjundiah, C.; Shimizu, K.; Osteryoung, R. A. *J. Electrochem. Soc.* **1982**, *133*, 1389.

(19) Baur, E. *Helv. Chim. Acta* **1925**, *8*, 403.

(20) Gutmann, V.; Gritzner, G.; Danksagmuller, K. *Inorg. Chim. Acta* **1976**, *17*, 81.

(21) Gritzner, G.; Danksagmuller, K.; Gutmann, V. *J. Electroanal. Chem. Interfacial Electrochem.* **1976**, *72*, 177.

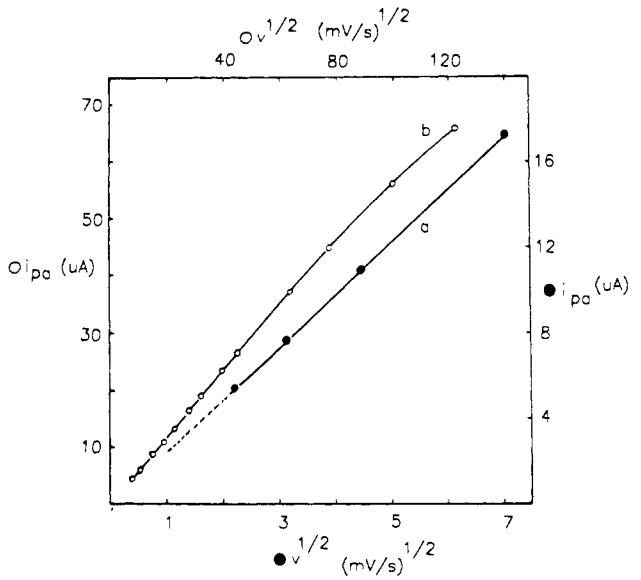


**Figure 6.** Anodic peak current ($i_{p_a}$) vs square root of scan rate ($v^{1/2}$) for $[(C_4H_9)_4N]_3Fe(CN)_6$ in 1.5:1 $AlCl_3$:ImCl melt: (a) $[(C_4H_9)_4N]_3Fe(CN)_6$ = 31.98 mM (linear scan; GC electrode ($r$ = 0.15 cm)); (b) $[(C_4H_9)_4N]_3Fe(CN)_6$ = 18.92 mM (staircase; W electrode ($r$ = 0.025 cm)).

The voltage shift for the ferrocyanide couple seen here is more than twice that and suggests a stronger Lewis acid interaction with ferrocyanide than with the $Fe(phen)_2(CN)_2$. (The potential shift is referred to that for the $Fe(CN)_6^{4-}/Fe(CN)_6^{3-}$ couple in water, which is +0.12 V vs the SCE;[22] the aqueous SCE potential is 60 mV negative with respect to the Al/Al(III), 2:1 melt reference,[23] using ferrocene/ferrocenium as an internal reference couple.[24])

Both the spectral features and the electrochemical behavior of the ferro/ferricyanide couple remained unchanged for $AlCl_3$:ImCl mole ratios of 1.5:1 to 1.2:1. The peak positions of the cyclic voltammograms were constant, but because of the negative shift of the anodic limit of the melt with a decrease of acidity, the voltammograms started to overlap with chlorine evolution and ultimately, at an acidity less than 1.2:1 $AlCl_3$:ImCl, no voltammetric behavior could be observed. Therefore, all electrochemical work was prepared in a melt of 1.5:1 $AlCl_3$:ImCl.

**a. Cyclic and Staircase Voltammetry.** The theoretical background of staircase voltammetry is well developed.[25] In this technique a constant-potential step ($\Delta E$) is applied for a period of time ($t$) and the current is sampled at some point during the step. The parameter $\Delta E/t$ in staircase voltammetry corresponds to the scan rate, $v$, in linear scan voltammetry. Figure 6a,b shows the change of anodic peak currents ($i_{p_a}$) with the square roots of the scan rates in cyclic and staircase voltammeries, respectively. Because of the proximity of the value of anodic peak potential of the couple to that of the chloride oxidation from the tetrachloroaluminate, it was rather difficult to measure precisely the cathodic peak currents. The cyclic voltammetry plot spans scan rates from 5 to 50 mV/s, and the staircase plot, scan rates from 50 to 15 000 mV/s. At scan rates from 5 to 50 mV/s the plot is linear and extrapolates to the zero of the axes. This indicates that the faradaic reaction is diffusion controlled and the homogeneous reaction between ferricyanide and tetrachloroaluminate is too slow to show any catalytic effect. The former conclusion is also supported by the $i_{p_a}$ vs $(\Delta E/t)^{1/2}$ plot (Figure 6b) of cyclic staircase voltammetry, where the diffusion-controlled behavior of the anodic reaction is obtained at least up to 6 V/s scan rate.

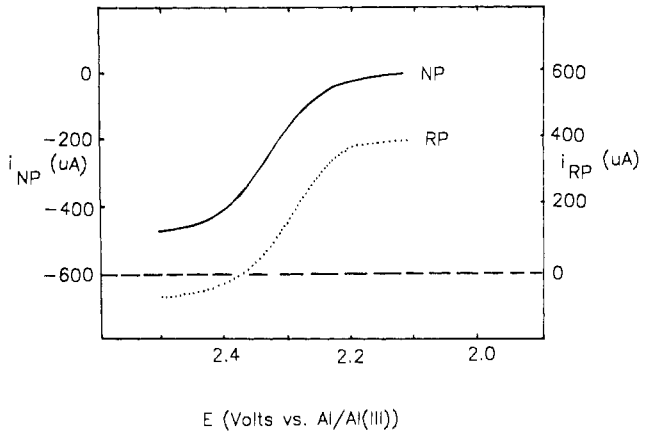


**Figure 7.** Normal- and reverse-pulse voltammograms of 31.98 mM $[(C_4H_9)_4N]_3Fe(CN)_6$ in 1.5:1 $AlCl_3$:ImCl melt (GC electrode ($r$ = 0.15 cm); pulse amplitude 10 mV; pulse width 25 ms; $E_{1/2}$(NP) = 2.33 V; $E_{1/2}$(RP) = 2.28 V).

The separation of the anodic and cathodic peak potentials with both techniques, even at the lowest scan rates, is found to be greater than 59 mV, the value for a reversible, one-electron-transfer process. At an electrode of radius 0.15 cm the $\Delta E_p$ for cyclic voltammetry increases from 70 to 105 mV as the scan rate changes from 5 to 500 mV/s, and the $\Delta E_p$ for staircase voltammetry, from 85 to 290 mV as the scan rate changes from 50 to 15 000 mV/s. However, at an electrode of smaller radius (W, $r$ = 0.025 cm) in the same solution, the corresponding peak separations with the cyclic staircase were from 68 to 122 mV. This suggests a large contribution from $iR$ drop in the peak separation. The $E_{p_a} - E_{p/2}$ values of the cyclic voltammograms at 10, 50, and 100 mV/s are 57, 60, and 64 mV, respectively, as against the reversible-couple value of $56.5/n$ at 25 °C. These results suggest that the $Fe(CN)_6^{3-}/Fe(CN)_6^{4-}$ couple is electrochemically quasi-reversible in the acidic $AlCl_3$–ImCl molten salt solvent.

**b. Normal- and Reverse-Normal-Pulse Voltammetry.** Both normal and reverse pulse are well-developed techniques.[26,27] In the former, potential pulses of successively increasing amplitude are applied to the electrode and the current is measured at the end of each pulse. Initially, the electrode potential is maintained at a value where no faradaic reaction occurs. The solution is stirred between pulses to renew the surface boundary conditions before the application of each new pulse. In the reverse-pulse mode, the electrode is stepped to a potential on the diffusion plateau of, in this case, the oxidation wave to generate a product or products, which are examined by pulses in the reverse direction.[27] In the diffusion-controlled region, the current obeys the Cottrell equation, $i_L = nFACD^{1/2}/(\pi t)^{1/2}$, where the terms have their usual meaning. When the redox couple is reversible, the normal- and reverse-pulse voltammograms are superimposable with the same $E_{1/2}$ values. Figure 7 shows normal- and reverse-pulse voltammograms of the couple under identical conditions. Although the general shapes of the curves are similar, the $E_{1/2}$ values are different; for the normal pulse $E_{1/2}$ is 2.333 V and for the reverse pulse it is 2.282 V. The difference of $E_{1/2}$ values between the two techniques decreases from 67 to 19 mV with an increase of pulse width from 16 to 100 ms, indicating a tendency toward reversible behavior at longer times. Similar behavior has been observed in the slopes of the $E$ vs log $[(i_L - i)/i]$ plots of the anodic scan at different pulse widths (data collected from normal-pulse voltammograms). For an increase of pulse width from 16 to 100 ms the slope changes from 84 to 68 mV/decade, while the value for a reversible couple should be 59 mV/decade. Figure 8 is a plot of $i_L$ vs $t^{-1/2}$ for the normal-pulse data. The plot is linear and passes through the origin, indicating a diffusion-limited process, and confirms that the anodic reaction is diffusion controlled within the time scale of the

(22) Bard, A. J., Parsons, R., Jordan, J., Eds. *Standard Potentials in Aqueous Solutions*; Dekker: New York, 1985; Chapter 19.
(23) Robinson, J.; Osteryoung, R. A. *J. Am. Chem. Soc.* **1979**, *101*, 323.
(24) Karpinski, Z.; Nanjundiah, C.; Osteryoung, R. A. *Inorg. Chem.* **1984**, *23*, 3358.
(25) Osteryoung, J. G.; Osteryoung, R. A. *Am. Lab. (Fairfield, Conn.)* **1972**, *4*(7), 8 and references therein.
(26) Osteryoung, J.; Kirowa-Eisner, E. *Anal. Chem.* **1980**, *52*, 62 and references therein.
(27) Sahami, S.; Osteryoung, R. A. *Inorg. Chem.* **1984**, *23*, 2511.

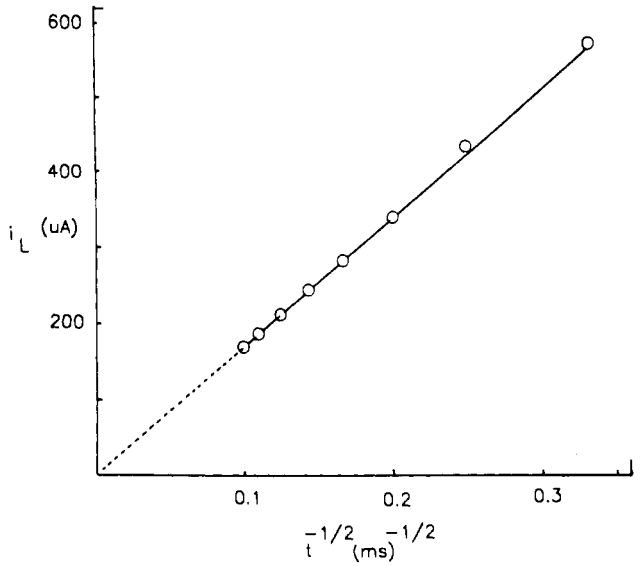


**Figure 8.** Limiting current ($i_L$) vs $t^{-1/2}$ for normal-pulse voltammetry of 31.98 mM $[(C_4H_9)_4N]_3Fe(CN)_6$ in 1.5:1 $AlCl_3$:ImCl melt (GC electrode ($r$ = 0.15 cm); pulse amplitude 10 mV).

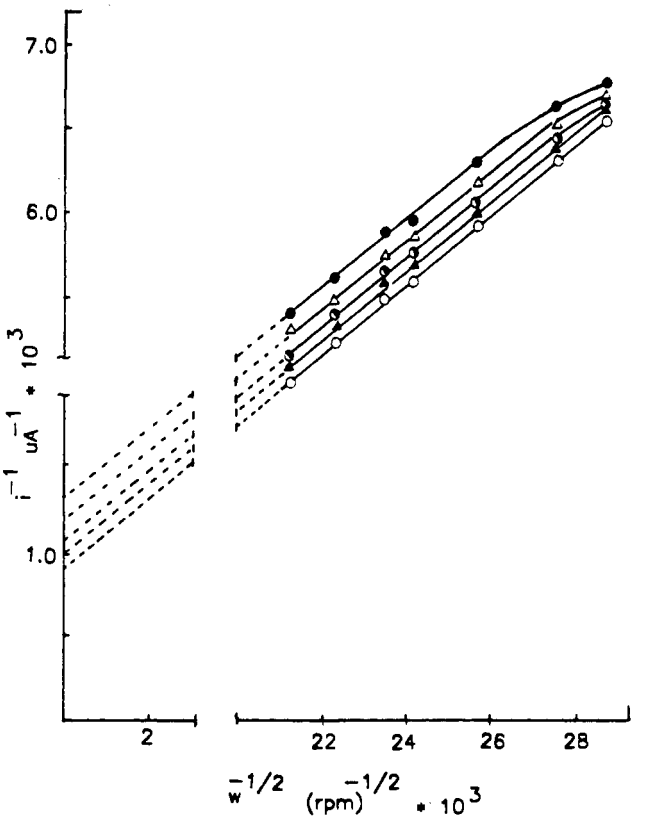


**Figure 9.** Plot of $i^{-1}$ vs $w^{-1/2}$ at (V vs Al reference) (○) 2.375, (▲) 2.370, (◑) 2.365, (△) 2.360, and (●) 2.355.

measurements. A plot of log $i_L$ vs log $t_p$ is linear with a slope of −0.5. The diffusion coefficient $D_R$, as calculated from the slope of the $i_L$ vs $t^{-1/2}$ plot, is $1.93 \times 10^{-7}$ cm$^2$/s. This value, although lower by about 1 order of magnitude from that in aqueous solution, is comparable to other values[18,27] in these molten salt solvents. Relative to that of water, the higher viscosity of the melt causes lower values of the diffusion coefficients of solutes in this system.[28]

**c. Kinetic Parameters.** The heterogeneous rate constant, $k^{o\prime}$, and the transfer coefficient, $\alpha$, of the $Fe(CN)_6^{4-}/Fe(CN)_6^{3-}$ couple have been determined by rotating-disk-electrode (RDE) voltammetry. The reciprocal of the current, $i^{-1}$, at different potentials,

(28) McLaughlin, E. *Trans. Faraday Soc.* **1958**, *55*, 28.

**Table II.** Kinetic Parameters from RDE Experiments[a]

| $E$, V | $10^3 i_k$, A | $10^3 k$, cm/s | $E$, V | $10^3 i_k$, A | $10^3 k$, cm/s |
|---|---|---|---|---|---|
| 2.355 | 0.741 | 1.905 | 2.370 | 1.000 | 2.575 |
| 2.360 | 0.833 | 2.137 | 2.375 | 1.111 | 2.860 |
| 2.365 | 0.909 | 2.343 | | | |

[a] 8 mM $(Bu_4N)_3Fe(CN)_6$ in 1.5:1 AlCl–ImCl melt; glassy-carbon RDE working electrode ($r$ = 0.4 cm); reference electrode Al(III)/Al in 1.5:1 AlCl–ImCl; scan rate 50 mV/s.

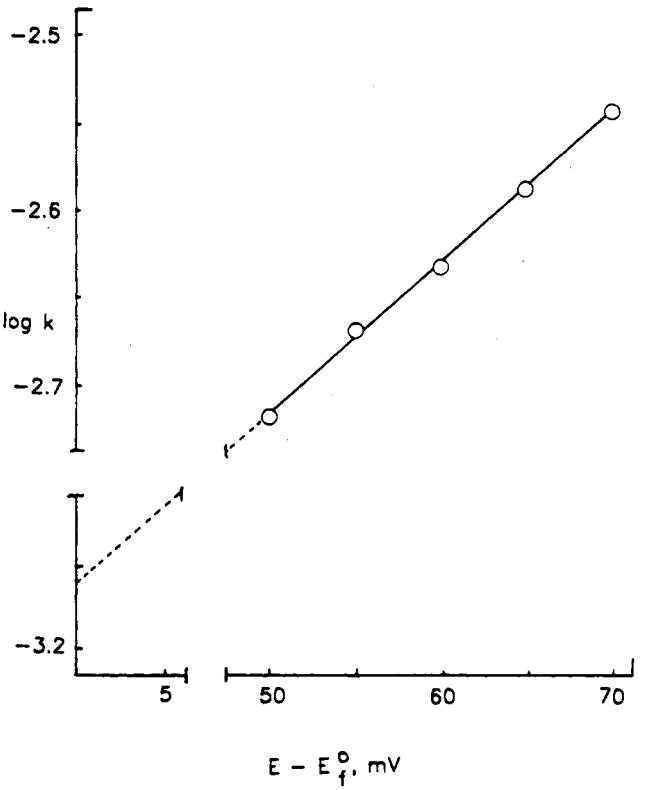


**Figure 10.** Plot of log $k(E)$ vs $E - E^{o}_{f}$ ($E^{o}_{f}$ estimated as +2.305 V (see text)).

$E$, in the kinetic region of the anodic scan was plotted against the reciprocal of the square root of the rate of rotation, $\omega^{-1/2}$ (Figure 9). From the Koutecky–Levich equation

$$1/i = 1/i_k + 1/0.62nFACD^{2/3}\nu^{-1/6}\omega^{1/2} \quad (1)$$

where $\nu$ is the kinematic viscosity and the rest of the terms have their usual meaning, the kinetic current, $i_k$, at a fixed potential was obtained from the intercepts of the plots. Rate constants as a function of $E$, $k(E)$, were calculated from the relation

$$i_k = nFA(k(E))C \quad (2)$$

and from the equation

$$k(E) = k^{o} \exp[[(1 - \alpha)nF(E - E^{o\prime})]/RT] \quad (3)$$

The formal rate constant, $k^{o\prime}$, and the transfer coefficient were obtained from the intercept and slope, respectively, of the log $k(E)$ vs $(E - E^{o\prime})$ plot (Figure 10). Table II summarizes the data. The $E^{o\prime}$ used in the plot is the formal potential of the couple $Fe(CN)_6^{4-}/Fe(CN)_6^{3-}$ obtained from the average of the peak potentials of the cyclic voltammogram at 50 mV/s scan rate and was 2.305 V. The values of $k^{o\prime}$ and $\alpha$ are $6.92 \times 10^{-4}$ cm/s and 0.48, respectively.

**Summary.** In the $AlCl_3$–ImCl molten salt solvent ferrocyanide forms adducts with $AlCl_3$ through the N of the C–N groups, as indicated by UV–vis and IR spectral data. The adduct formation stabilizes the ground state of Fe(II) and increases the oxidation potential of the complex by about +2 V relative to that in water. Cyclic voltammetric experiments in the 1.5:1 $AlCl_3$:ImCl melt result in anodic and cathodic currents with peak potential sepa-

ration of about 75 mV at a scan rate of 50 mV/s. The voltammogram has been attributed to the $Fe(CN)_6^{3-}/Fe(CN)_6^{4-}$ couple. The formal potential of the couple, calculated from the voltammogram, is more positive than the potential for chlorine evolution from the tetrachloroaluminate ion in the melt. Thus, ferricyanide is thermodynamically unstable, but the homogeneous reaction is too slow to produce any observable catalytic anodic current under our experimental conditions. The couple undergoes a quasi-reversible faradaic reaction that is diffusion controlled. No electroactivity of the couple was observed in neutral or basic melt, as the couple is insoluble.

**Acknowledgment.** This work was supported by the Air Force Office of Scientific Research.

**Registry No.** $(Bu_4N)_3Fe(CN)_6$, 14589-06-1; $(Bu_4N)_4Fe(CN)_6$, 53682-43-2; 1-methyl-3-ethylimidazolium chloride, 65039-09-0; aluminum chloride, 7446-70-0; tetrachloroaluminate, 17611-22-2; potassium ferricyanide, 13746-66-2.

---

Contribution from the Institut für Anorganische Chemie, Universität Basel, Spitalstrasse 51, 4056 Basel, Switzerland

# Coordination Geometries of Hexaamine Cage Complexes

Peter Comba

*Received June 13, 1988*

The structures of all six important conformers of the first-row transition-metal hexaamine cage complexes $M(sar)^{n+}$ (sar = 3,6,10,13,16,19-hexaazabicyclo[6.6.6]eicosane) have been computed by strain energy minimization calculations with fixed M-N distances between 1.90 and 2.36 Å. The excellent agreement between calculated and experimental structural parameters supports the force field used, which involves replacing metal-donor atom angle deformation terms by nonbonded interactions between the donor atoms. From the analysis of the total strain energy in dependence of M-N for all conformers considered, the following points emerge: (i) For small M-N distances (M-N < 2.0 Å) five conformers have similar strain energies; viz., their relative stability is dependent on environmental factors (crystal lattice, solution media, etc.), and this is in agreement with experimental data. (ii) With increasing number of oblique en-type chelate five rings (*ob* conformations) the stability decreases with increasing size of the metal centers. $lel_2ob$, $ob_2lel$, and $ob_3$ conformations are unstable vs the $lel_3$ conformations for M-N > 2.0, 2.10, and 2.2 Å, respectively. Qualitatively, this was already assumed from experimental data; however, it has not been quantified yet. (iii) Above ~2.2 Å there exists only one conformation with $D_3lel_3$ geometry. This conformation is different from the $D_3lel_3$ conformation observed for smaller M-N distances (e.g. cobalt(III) cages), and it has not been identified before. (iv) The analysis of the structural parameters of $M(sar)^{n+}$ in dependence on M-N indicates that the unsteady course of the twist angle $\phi$ vs M-N is the result of conformational changes. Metal-centered electronic effects in relation to these structural factors are also briefly discussed.

## Introduction

Molecular-mechanics calculations are now relatively well established in coordination chemistry.[1] A large part of the studies deals with cobalt(III) hexaamines, and it is often tedious and difficult to get accurate force field parameters for other systems. With the recent improvement[2] of the widely used force field for cobalt(III) hexaamines,[3] the only metal-dependent force field parameters are the two parameters ($k$ and $r_0$) that describe the metal center-ligand atom (M-N) breathing mode. One aim of the present study was to test the quality of these changes based on a large amount of experimental data. Furthermore, for a recently started project, which involves the design by molecular mechanics calculations of ligands used for stereoselective ligand exchange on chiral matrices,[4-6] it was also important to test these recently proposed changes.

A large number of transition-metal hexaamine cage complexes with sar-type ligand systems are known (sar = 3,6,10,13,16,19-hexaazabicyclo[6.6.6]eicosane; for atom labeling, see Figure 1). The most prominent structural variation in the whole series is the trigonal twist angle $\phi$, which varies from about 25 to roughly 60° (for definitions of structural parameters, see also Figure 1). In a recent publication we have analyzed the variation of the twist angle $\phi$ based on a ligand field model.[7] I am now presenting metal center independent strain energy minimization calculations of all six important conformers of $M(sar)^{n+}$. Minimized strain energies and structural parameters are analyzed as a function of the M-N bond length ("blowing up" of the cages), and the calculated parameters are compared with experimental data. This analysis is discussed in relation to the quality of the presently used force field, to the possible evaluation of force field parameters for metal centers other than cobalt(III), and to the question of the influence of metal-centered electronic effects toward the structure of the cage complexes.

## Experimental Section

In the molecular-mechanics formalism the structure of a complex is calculated by strain energy minimization. The total strain energy (conformational energy) is parametrized into bond length ($E_b$), valence angle ($E_\theta$), torsion angle deformation ($E_\phi$), and nonbonded interaction energies ($E_{nb}$):

$$U_{total} = \sum(E_b + E_\theta + E_\phi + E_{nb}) \quad (1)$$

$$E_b = \tfrac{1}{2}A_b(r - r_0)^2 \quad (2)$$

$$E_\theta = \tfrac{1}{2}A_\theta(\theta - \theta_0)^2 \quad (3)$$

$$E_\phi = \tfrac{1}{2}A_\phi(1 + \cos 3\phi) \quad (4)$$

$$E_{nb} = A_{nb}[\exp(-Bd)] - C/d^6 \quad (5)$$

All strain energy minimization calculations have been performed with the Fortran program MOMEC85.[8] It involves a modified Newton-Raphson technique that allows for simultaneous variations in all coordinates. All calculations are based on a recently developed force field parametrization,[2] which is widely used for cobalt(III) hexaamines. As usual, the strain energy minimized structures and all strain energies are the result of the optimized structures of the "naked" complex ion; viz., environmental effects such as solvation, ion pairing, and crystal lattice effects are not included.

The force field used involves representing valence angle bending terms between the metal center and two ligating atoms (N-M-N) by nonbonded interactions between the ligating atoms N. Therefore, the only metal center dependent parameters are related to the M-N breathing mode (M-N-X angle functions are assumed to be metal center M independent). The M-N dependent structural parameters and strain en-

(1) Brubaker, G. R.; Johnson, D. W. *Coord. Chem. Rev.* **1984**, *53*, 1.
(2) Hambley, T. W.; Hawkins, C. J.; Palmer, J. A.; Snow, M. R. *Aust. J. Chem.* **1981**, *34*, 45.
(3) Snow, M. R. *J. Am. Chem. Soc.* **1970**, *92*, 3610.
(4) Comba, P.; Hambley, T. W.; Zipper, L. *Helv. Chim. Acta*, in press.
(5) Comba, P.; Maeder, M.; Zipper, L. Submitted for publication.
(6) Comba, P.; Zipper, L. Work in progress.
(7) Comba, P.; Sargeson, A. M.; Engelhardt, L. M.; Harrowfield, J. MacB.; White, A. H.; Horn, E.; Snow, M. R. *Inorg. Chem.* **1985**, *24*, 2325.
(8) Hambley, T. W. "MOMEC85, a Fortran program for strain energy minimization"; Department of Chemistry, The University of Sydney, Australia.

0020-1669/89/1328-0426$01.50/0 